IRSTI 41.51.31; 37.15.15 https://doi.org/10.26577/phst20261314

Near-infrared imaging of the twilight sky: enhanced detection of noctilucent and high-altitude clouds

A.A. Solodovnik, T.B. Kasenov, P.I. Leontyev, B.M. Useinov* and N.P. Solodovnik

Manash Kozybayev North Kazakhstan University, Petropavl, Kazakhstan
*e-mail: buseinov@gmail.com

(*Received March 31, 2026; received in revised form May 18, 2026; accepted May 28, 2026*)

As part of efforts to improve the methodology for detecting and monitoring noctilucent clouds (NLCs), observations of the twilight sky conducted during the summer season of 2025 were analyzed. The study examines existing approaches to NLC imaging and demonstrates that the information content of ground-based observations can be significantly enhanced through increased image contrast. To achieve this, observations were extended from the visible spectral range to the near-infrared (NIR) region using a modified CANON 1000D camera with enhanced NIR sensitivity and a set of interchangeable optical filters. For the first time, simultaneous monitoring of the twilight sky was performed using two cameras operating in different spectral ranges: a modified CANON 1000D in the near infrared and a CANON 2000D in visible light. Observations carried out from late May to early September 2025 revealed a substantial increase in image contrast in the NIR region compared with conventional visible-light imaging. The obtained results demonstrate the advantages of near-infrared observations for the detection and analysis of noctilucent clouds and other atmospheric phenomena under twilight conditions. The proposed approach expands the capabilities of ground-based optical monitoring and provides a basis for further development of observational techniques for upper-atmosphere studies.

Keywords: twilight segment, noctilucent clouds, image contrast, infrared camera, infrared imaging, cloud monitoring.

1. Introduction

In standard astronomical research practice, objects are observed in the dark night sky, with the notable exception of solar studies. However, there are phenomena and objects observed within the twilight (or auroral) segment of the celestial sphere. Besides bright celestial bodies such as Venus and Jupiter (which are the first to appear in the evening sky), these include, primarily, noctilucent and nacreous clouds. Occasionally, phenomena such as zodiacal light and the gegenschein are also attributed to this category [1-3].

In atmospheric optics and astronomy, twilight refers to strictly defined time intervals after sunset or before sunrise. During twilight, the solar disk is not visible above the horizon, yet the celestial sphere is illuminated by radiation scattered by the atmosphere. The level of illumination is determined by the altitude of the center of the solar disk, i.e., the angle at which the Sun has dipped below the horizon. Based on the depression angle, twilight is classified into civil (from 0° to -6°), nautical (from -6° to -12°), and astronomical (from -12° to -18°). When the Sun dips below -18°, "astronomical night" begins, at which point sunlight scattered by the upper atmospheric layers practically ceases to affect astronomical observations [4-6].

The part of the celestial sphere illuminated by solar radiation scattered by overlying atmospheric layers is called the twilight segment. It is clearly visible to the naked eye as an arc-shaped bright region stretched along the azimuth above the point where the Sun has set below the horizon. It is bounded at the top by the dark band of the Earth's shadow and at the bottom by the horizon line. The altitude of the upper boundary of the twilight segment changes continuously, descending in the evening and ascending in the morning. The formation of the twilight segment is associated with the scattering of solar rays in the upper atmospheric layers (mainly in the stratosphere) [4-6]. The twilight segment is observed particularly distinctly under conditions of minimal dust and high tropospheric humidity, for example, after rainy weather. Conversely, its visibility is negatively affected by lunar illumination (near a full moon) or bright artificial light sources (urban environments). Latitudinal and seasonal factors also significantly influence the duration of twilight [4-6].

The first of the aforementioned objects that stand out specifically against the background of the twilight part of the sky are NLC. Photometric visibility conditions are exceptionally important for them. These clouds are completely invisible in the daytime sky due to their exceptionally low contrast against the sky background, which is caused by a low aerosol concentration within them, and consequently, weak scattering of solar radiation [7, 8]. An exception is total solar eclipses, during which the background sky brightness drops sharply so that stars become visible. It should be noted that the visibility of stars in the sky is a significant photometric marker of the background sky brightness required for the visual observation of NLC. Such conditions occur at the boundary between civil and nautical twilight; however, with the transition from nautical to astronomical twilight, the visibility of NLC sharply deteriorates due to a decrease in their illumination by solar rays.

As for zodiacal light, caused by the scattering of solar radiation on interplanetary dust particles, the conditions for its observation are generally similar to those characteristics of NLC. However, unlike the latter, this glow is observed only at a relatively small angular distance from the Sun, which is explained by the features of the spatial distribution of the scattering particles. A phenomenon such as the gegenschein, due to its extremely low brightness, is observed only under conditions of astronomical night, unlike zodiacal light [6].

Often, objects observed in the twilight segment are comets. Indeed, as comets approach the Sun, they rapidly increase their brightness, which reaches its maximum (in absolute magnitude) near the epoch of their perihelion passage.

Thus, observations of a variety of celestial objects and phenomena for which there is expressed scientific interest are highly relevant within the twilight segment region.

2. Features of ground-based registration of high-altitude clouds

To date, there are two comprehensive approaches to obtaining information about the state of NLC fields: studying them using orbital spacecraft and ground-based observations. Despite all the undeniable advantages of studying NLC from space (primarily due to the elimination of weather effects), ground-based methods for investigating them have not lost their relevance. The reason for this lies not only in the episodic nature of space missions but also in the variety of experimental approaches that can be utilized when studying NLC from the Earth's surface. Examples of the most significant scientific achievements associated with ground-based NLC observation methods include the development of a morphological classification of cloud forms, estimates of aerosol microphysical parameters, and conclusions regarding the relationship between the evolution of NLC fields and meteorological processes in the troposphere [2, 7-10].

In particular, one of the most important tasks in studying NLC and their connection to atmospheric processes is registering the very fact of the presence of mesospheric clouds at a given time and in a given location. Such observations are called synoptic, and they are currently conducted using digital cameras, often operating in automatic mode. Obtaining data on the presence (or absence) of NLC allows for a more precise understanding of the influence of various physical factors of terrestrial or cosmic origin on the state of the upper atmosphere [9-14].

As an example of the importance of obtaining such data, one can point to the operation (since 2004) in the Northern Hemisphere of a network of digital automatic cameras for registering NLC and studying their spatiotemporal dynamics [15]. This network, called Network of Automatic Photographic Survey of NLC, includes observation points located along a latitudinal circle (53–56° N), which allows for comparable NLC observations. This creates conditions of identical illumination of the twilight segment by the Sun and similar physical conditions in the mesopause (temperature and wind speed within it depend on geographic latitude). The first scientific results based on this network measurements were published in the work of Dalin et al. [16].

The obtained data made it possible to trace the propagation of atmospheric planetary waves with periods of two and five days. Propagating into the region where NLC can form, they affect the frequency and brightness of their appearance. Specifically, during the 2006 and 2007 seasons, two-day planetary waves influenced NLC activity to a greater extent than five-day waves [13]. Furthermore, it was found that the influence of planetary waves on NLC brightness variations is small, with their average contribution being 3–5%.

Naturally, the first and most serious obstacle to synoptic NLC observations is tropospheric cloudiness, the density of which increases toward the horizon. However, clouds are not the only hindrance to NLC registration. The season of NLC fields evolution covers the period from the end of May to the beginning of August, and in the summer period the dustiness of the ground layer of air increases noticeably. Scattering by atmospheric dust aerosols significantly reduces the visibility of NLC at low altitudes above the horizon. Additionally, the question logically arises of expanding the temporal window for NLC registration, for instance, making it accessible immediately after sunset. This requires reducing the background brightness of the twilight sky.

Solving this latter task would increase the efficiency of registering not only NLC but also nacreous (stratospheric) clouds, and raise the possibility of registering other poorly studied forms of high-altitude clouds.

3. Methodology of IR monitoring of the twilight segment

A typical program for synoptic NLC observations is fairly simple. It involves obtaining a series of images of the twilight segment with the widest possible azimuth viewing angle. The need for a wide field of view is dictated by the potential appearance of NLC, for example, in the evening from the west to the north. When using wide-angle optics in manual mode, a single camera is quite sufficient. For automated observations with stationary cameras throughout the night, two cameras will be required. Imaging is conducted from the end of civil twilight in the evening until its onset in the morning. Usually, these times are calculated in advance for each day of the season; however, there are situations when NLC are clearly visible in the mornings even under civil twilight conditions. The interval between shots can vary from 1 to several minutes.

Typically, digital cameras have a spectral sensitivity maximally approximated to that of the human eye. In this case, all the aforementioned limitations on NLC visibility remain valid. In some sources [2], there are recommendations regarding the use of optical filters selecting the blue-cyan wavelength region when taking NLC images. It can be assumed that these are based on the consideration that NLC aerosols most effectively scatter visible radiation specifically in these colors. Consequently, one might expect an increase in the contrast of NLC images in the photographs. However, one should not forget that air molecules also have maximum scattering efficiency at the same wavelengths (which, in particular, determines the color of the sky). For this reason, and due to the fact that conventional black-and-white photographic films had a sensitivity peak in blue-cyan rays, the application of such techniques did not see further development [2].

It is possible to increase the contrast of NLC images in twilight segment photographs using another method. Specifically, by significantly reducing the sky background brightness. To achieve this, it is sufficient to transition from imaging the sky in the visible range to photographing in the near-IR spectral region [17, 18].

Isolating the required wavelength range is not complicated due to the availability of a wide selection of good-quality optical light filters. Unfortunately, conventional cameras practically do not detect radiation with a wavelength longer than 750 nm. This is because camera manufacturers deliberately restrict the sensitivity range to the visible region to enhance image sharpness. This is achieved by installing a corresponding glass filter over the surface of the radiation receiver. Figure 1 presents the wavelength dependencies of the transmittance for the digital camera sensor, the glass light filter in front of it, and the camera lens.

As can be seen, the transmittance of the glass filter in front of the sensor excludes the entry of radiation with a wavelength longer than 740 nm, despite the sensor itself possessing good sensitivity in the region up to 1000 nm. The residual sensitivity of cameras in the near-IR spectral region requires exposures of several seconds under daylight conditions and no less than 5 minutes under twilight conditions [17, 18]. Such long exposures are unacceptable for implementing the NLC monitoring task.

The sensitivity of a digital camera to IR radiation can be significantly increased (by 2-3 orders of magnitude) by removing the aforementioned light filter. This was done for the CANON 1000D camera [17] in the in a specialized optical workshop. The general view of the camera and its schematic diagram are shown in Figure 2.

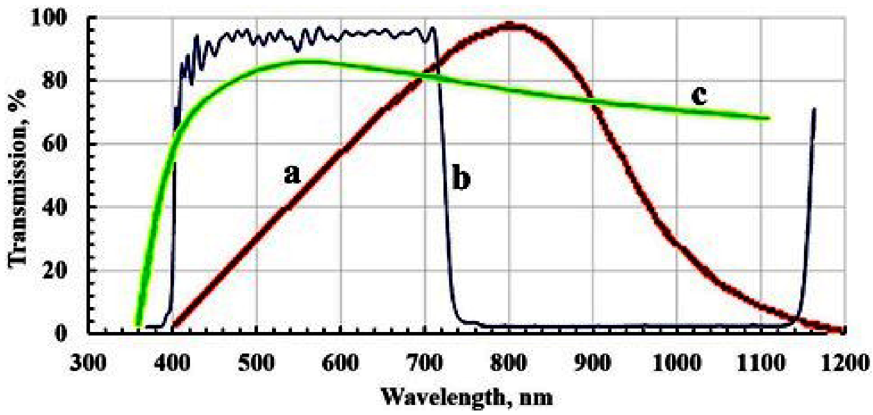

Figure 1. Wavelength dependence of the light transmittance for:
a) the digital camera sensor; b) the camera's glass light filter; c) the camera lens.

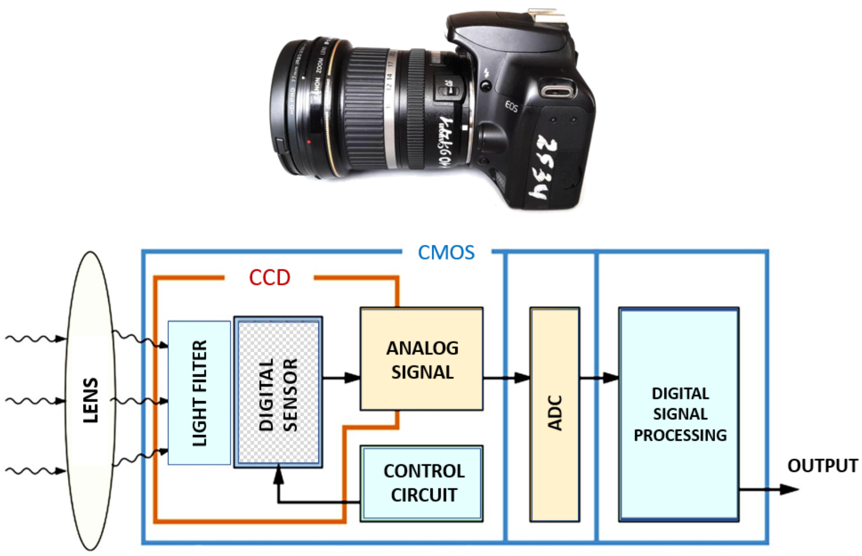

Figure 2. General view of the CANON 1000D camera and its schematic diagram [19]
The light filter is removed when the camera is modified.

Test shots using RG780, RG830, and RG850 IR filters (where the numbers indicate the start of the transmission band in nm) confirmed a hundredfold increase in camera sensitivity under identical aperture settings and specified sensor sensitivity.

The overall goal of monitoring the twilight segment was to compare the quality and information content of sky images in the visible and near-IR spectral regions (RG850 filter), as well as to conduct a general analysis of NLC registration efficiency in the IR spectral region. For the first time in the practice of studying NLC, filming was carried out using two cameras: CANON 2000D [21] in visible light and a modernized CANON 1000D in the near IR wavelength region. The cameras had identical CANON EF-S LENS wide-angle lenses. Photographing was carried out at the exact same moments in time (with an accuracy of up to 5 seconds). Camera sensitivities were set to ensure comparable exposure durations. It should be noted that obtaining an infrared image of the twilight segment at the end of nautical twilight at an ISO value of 1600 required an exposure of approximately 25-30 seconds at an aperture of 4.5. Observations were conducted in the evening from the beginning of June to September 2025 in the city of Petropavlovsk (54.87°N, 69.13°E) facing west with a virtually completely open horizon. The shooting was conducted manually with the cameras mounted on tripods. The total number of observation nights was 41, with the number of images suitable for subsequent analysis being 474, of which 356 were in the IR range. Detailed monitoring information is provided in Table 1. Gaps in dates correspond to nights with overcast (rainy) weather.

Table 1. General information on NLC monitoring in the 2025 season.

№	Date	Time	Weather conditions	Presence and type of NLC
1	05.27	22:00 22:40	Clear	Bands parallel to the horizon from the west-northwest to the north. Five degrees below Capella.
2	05.28	-	Low clouds	None
3	05.30	-	Cloudy	None
4	05.31	-	Cloudy	None
5	06.02	22:15 22:45	Clear	Faint NLCs. Five degrees above Capella. From the west-northwest to the north. Veil and bands.
6	06.03	-	Cloudy	-
7	06.04	-	Cloudy	IR images taken.
8	06.06	-	Cloudiness	None
9	06.07	-	Cloudiness	None
10	06.08	-	Light cloudiness	None
11	06.09	-	Light cloudiness	None
12	06.10	-	Light cloudiness	None
13	06.11	-	Clear	None
14	06.14	22:10 22:55	Clear	Faint, low bands in the direction from the west initially, moving to the north by 23:20.
15	06.15	-	Clear	None. Images taken.
16	06.16	-	Clear	None. Images taken.
17	06.19	22:00 22:42	Clear	Clouds are not visible visually, but the IR camera records them as filaments in the northwest direction at an altitude of 10-15 degrees.
18	06.21	-	Partly cloudy	None
19	06.22	22:20 22:37	Cloudiness	Presence of NLCs is noticeable.
20	06.25	21:40 22:25	Clear	Unusual clouds. Recorded by the IR camera, but not by the conventional camera. Rapid movement. Possibly cirrus clouds.
21	06.26	-	Clear	None
22	06.27	-	Clear	None
23	06.28	-	Clear	No NLCs in the evening sky. NLCs observed in the morning in Poludino.
24	06.29	-	Cloudy	None
25	06.30	-	Clear 0%	None
26	07.01	-	Clear 0%	None
27	07.02	-	Cloudy	None
28	07.04	-	Cloudy	Photographs taken.

Continuation of the table

№	Date	Time	Weather conditions	Presence and type of NLC
29	07.05	-	Cloudy	Photographs taken.
30	07.07	21:50 22:57	Partly cloudy	Not recorded by the IR camera, but captured by the conventional camera. Lunar illumination?
31	07.08	-	Cloudy	Photographed with two cameras. No NLCs.
32	07.14	21:46 22:27	Cloudy	Photographed with two cameras. No NLCs.
33	07.15	21:25 22:39	Clear	Formations resembling NLCs. Images taken with two cameras.
34	07.16	-	Clear	None
35	07.17	-	Clear	None
36	07.19	-	Clear	None
37	07.20	-	Clear	None. Photographs taken.
38	07.28	-	Cloudy	No NLCs. Photographs taken.
39	07.29	-	Cloudy	Photographs taken.
40	07.30	-	Cloudy	Images of lightning.
41	08.01	-	Cloudy	Interesting vortex.

Unfortunately, the number of nights in which NLC appeared during the 2025 season was small. It should be noted that the comparative rarity of NLC occurrences this season was also documented by other observers in the Northern Hemisphere. This circumstance is associated not with unfavorable weather conditions, but most likely with the physical influence of solar activity factors. As is known, the intensity of NLC formation can anti-correlate with solar activity indices [21-23].

4. Analysis oof twilight segment data in two spectral regions

Figure 3 presents examples of fragments of paired twilight segment images obtained during the study. Here, the IR images are presented in black and white. The dates and times of image acquisition are indicated.

Upon general review of the images, their substantial difference is noticeable. For example, LED lamps on the building roof are practically invisible in the IR images, which, however, is not surprising. Much more important are the sharp differences in cloud structure. In the upper and lower rows, details of cirrus and stratiform clouds that are barely distinguishable in the visible range are drawn with high contrast down to fine structural details in the IR region. In the middle row images, cloudiness in the visible range is virtually absent in the upper and central parts of the image, but it is clearly distinguishable (as cirrus clouds) in the IR rays.

Of particular interest is the comparison of images in which NLC are present (typically identified visually in the sky). Figure 4 provides a comparison of one such pair.

At the time of imaging (nautical twilight), the Sun was located at an altitude of -9.5° below the horizon. A simple visual comparison of the images appears to be quite challenging. While faint NLC bands are quite distinctly visible in the visible-light image, they are not as clearly traced in the IR region image. At the same time, cloud details in the upper left part are displayed with prominent relief in the IR image, whereas they are completely absent in the visible light image. A certain degree of clarity in the qualitative comparison of the informational value of the two approaches can be provided by determining the contrast coefficients of these and other images.

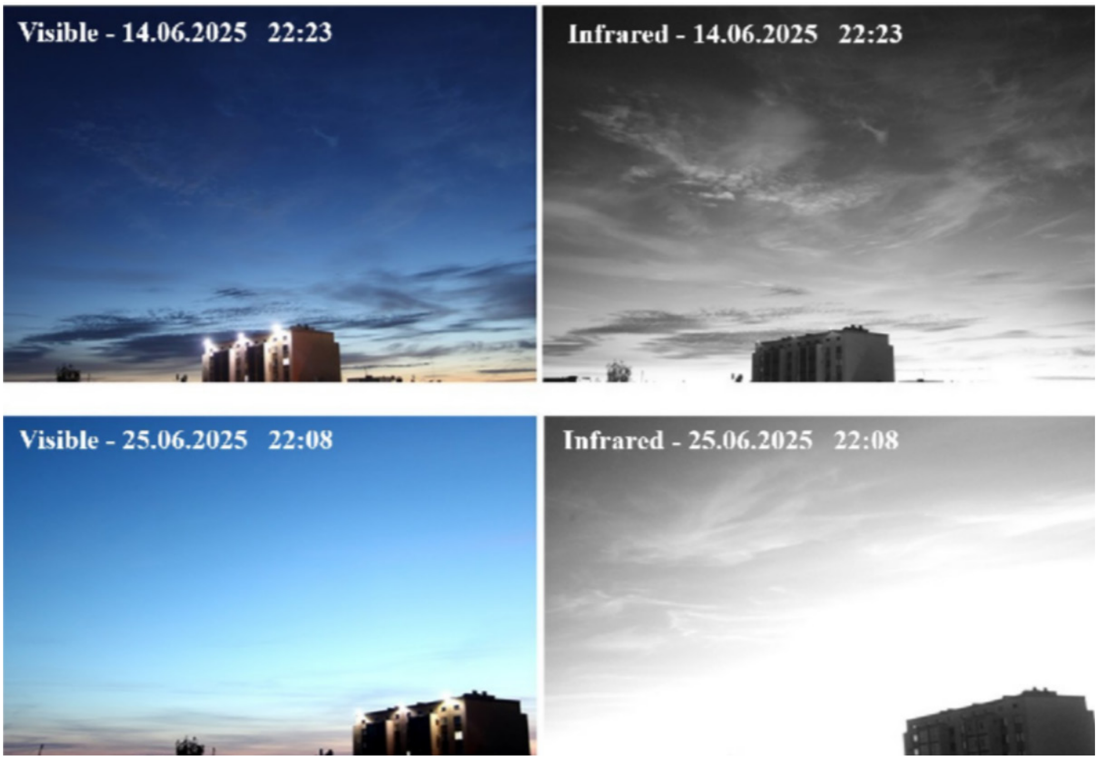

Figure 3. Examples of twilight segment images in the visible spectral region (left) and in the near-IR range (λ ≥ 850 nm, right).

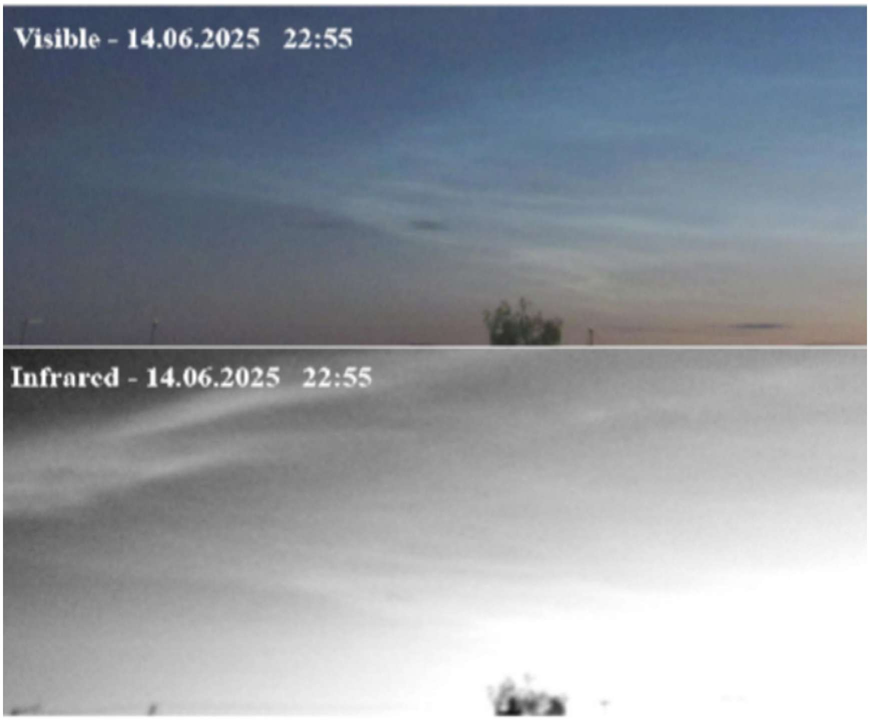

Figure 4. Twilight segment images where NLC are present.

5. Quantitative assessment of image information content

To assess the contrast of the twilight segment images, a method based on calculating the root-mean-square deviation (RMSD) of brightness was used. The method is implemented in available software programs [24-27]. Fundamental to this method is the principle that the greater the spread (variation) in pixel brightness values in an image, the higher the contrast. Here, the RMSD is precisely the mathematical measure of the spread of brightness values. In this procedure, the average brightness of all pixels is calculated for a given image area. Next, the difference between each pixel's brightness and the average value is determined. These values are squared, summed, divided by the number of pixels, and the square root is extracted from the result.

The result obtained is the standard deviation for the brightness of image pixels σ. The global contrast for the entire image was calculated using the formula:

$$K_{\text{г}} = \frac{2\sigma}{G-1}.$$

Processing of images to obtain a quantitative assessment of their quality (contrast) was performed using the ImageJ software package [29]. This program, in particular, allows one to obtain histograms of pixel brightness distribution across an image field and, if necessary, achieve local contrast enhancement. An example of processing and subsequent comparison of the results is shown in Figure 5.

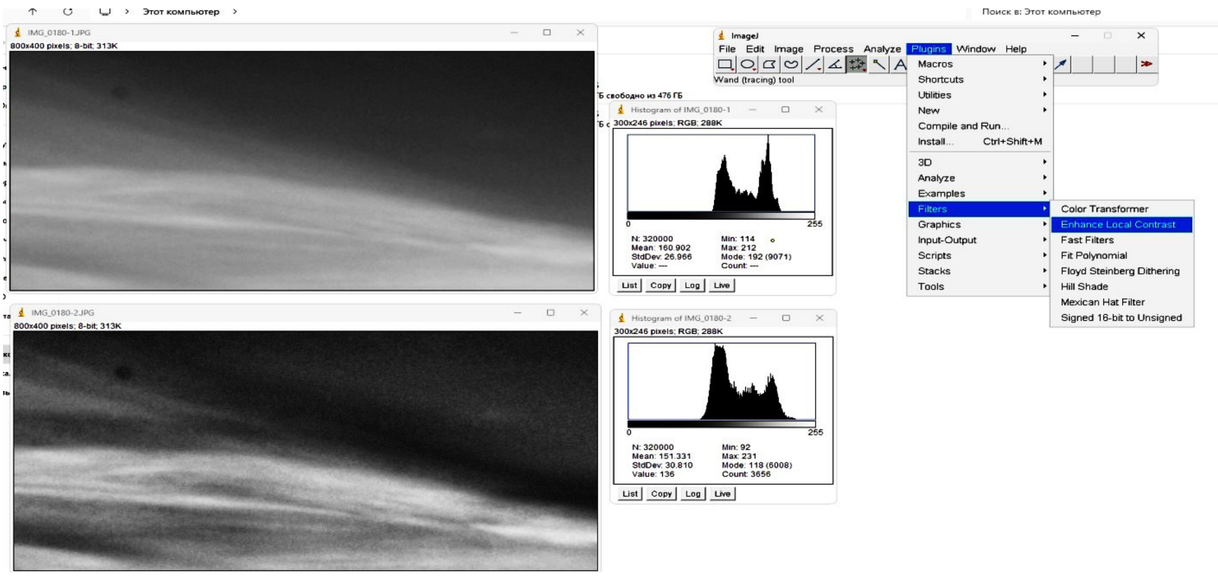

Figure 5. Example of image analysis and processing in ImageJ software.

When comparing the contrast of the photographs, the images were converted to a single 8-bit format. Using ImageJ software, identical objects were highlighted in both photographs, visible against the twilight sky. Exposure times for both cameras were selected to be as close as possible, with the difference in shooting times not exceeding 5 seconds. Table 2 provides examples of calculating the RMSD (σ) of pixel brightness for a series of twilight segment images in the visible range and in the near-IR spectral region.

As is easily observed, the change in cloud image contrast in the twilight segment upon transitioning from imaging in the visible spectral region to the near-IR region is positive throughout. At the same time, the spread of contrast change values is quite significant. A prime example of this is illustrated by the images from July 28, 2025 (Fig. 6).

Table 2. Comparison of image contrast in visible light and in the near-IR region.

Date of shooting	The visible region of the spectrum		The IR region of the spectrum		Changing the contrast, %
	Img_№	σ1	Img_№	σ2	(σ2-σ1)/ σ1
14.06	7008	23.5	0470	26.8	+ 14
	7011	19.5	0471	29.2	+ 50
	7014	15.7	0473	27.9	+ 78
25.06	0127	40.5	0534	49.3	+ 22
7.07	0168	46.0	0628	51.1	+ 11
14.07	0191	35.2	0655	51.4	+ 46
15.07	0201	31.0	0674	39.3	+ 27
28.07	0208	15.9	0700	35.7	+ 124
	0209	11.8	0705	13.3	+ 13
01.08	0210	35.6	0719	48.0	+ 35
	0213	28.2	0721	53.8	+ 91
	0215	22.2	0722	32.7	+ 47
	0216	13.1	0723	15.7	+ 20
Mean					+44

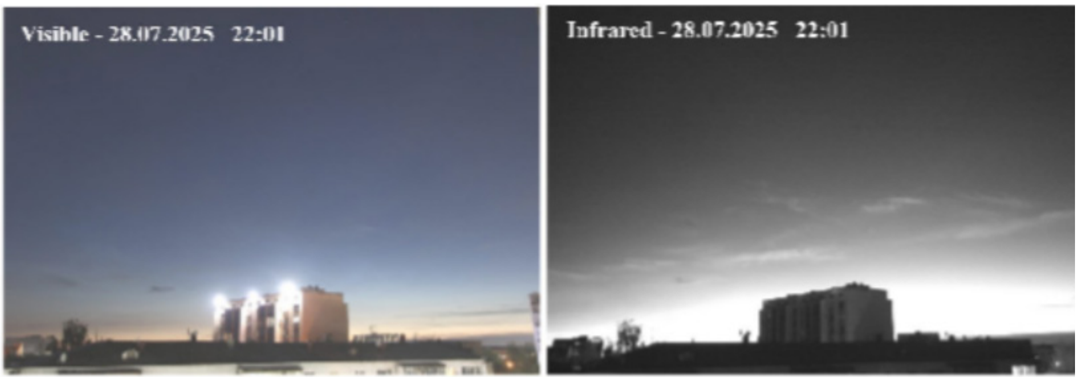

Figure 6. Twilight segment images with the greatest difference in contrast between the visible and IR ranges.

The cloudiness visible in the IR spectral region in Figure 4 may represent one of the high-altitude forms, including NLC. For now, one can only assume that the magnitude of the contrast change can be influenced by two external factors and one technical parameter. Firstly, the differences in the type of cloudiness in images taken on different dates, and secondly, differences in the altitude of the Sun below the horizon. Regarding the latter, this refers to the influence of the ratio between the camera sensitivity set during shooting and the exposure duration. As is known, high ISO values reduce image contrast, but it is difficult to avoid their use when imaging in the IR range due to the noticeably lower sensor sensitivity and much weaker radiation fluxes. In the perspective of further method refinement, these circumstances will need to be taken into account.

6. Examples of atmospheric objects and phenomena in the IR region

The abundance of material obtained during monitoring made it possible to identify interesting examples related to the specificities of operating in the IR range. Some of them warrant separate consideration.

For instance, on the night of July 29, a distant thunderstorm front was observed in the southwestern part of the twilight segment. Subsequently, analysis of the images revealed the presence of lightning discharges (Fig. 7).

In principle, this is not surprising. What is noteworthy is the fact that lightning is confidently discernible through the cloud medium on IR images, whereas on standard images or during visual observation, only an increase in the brightness of the cloud field is recorded.

Figure 7. Image fragment with a lightning discharge in the IR range.

In a number of cases, cloud formations that are completely inaccessible to the naked eye (whose contrast sensitivity is higher than that of conventional photography, making the sky look absolutely clear to the eye) are noticeable on IR images. An example is shown in Figure 8.

imilar situations were repeatedly recorded by the cameras. Thus, Figure 9 shows that in cases where images from a conventional camera (or visual observations) do not detect the presence of cloudiness in the sky, clouds may be present on images in the IR range. Identifying the cloud type in these cases can sometimes be quite difficult.

Figure 8. IR image of cloudiness in the form of filaments in the northwest direction at an altitude of 10-15 degrees, which are visually indistinguishable.

Structurally, the cloud field in the image obtained by the IR camera resembles one of the most transparent types of cirrus clouds (Ci fib or Cs fib). However, unlike the indicated cloud forms, they moved much faster, traveling in a southwestern direction. Such rapid movement is characteristic of high-altitude cloud types if they form in the uppermost layers of the troposphere or in the stratosphere at altitudes of 11–14 km [6, 29].

Figure 9. Cloudiness recorded only by the IR camera.

However, opposite situations were occasionally encountered, where a conventional camera recorded cloud details, while they were absent in the IR images. This occurred when there was an almost full Moon in the sky (Fig. 10).

Such situation can be explained by the attenuation of the IR component in the lunar spectrum compared to solar radiation. In this case the Moon lights cirrus clouds in the visible region of the spectrum even beyond the twilight segment. Inexperienced observers might mistake such view for NLC.

The high contrast of IR images sometimes completely alters the appearance of cloudiness compared to the picture in the visible spectral region. A striking example of this can be seen in Figure 11.

Figure 10. Illumination of cirrus clouds by a full Moon.

Figure 11. S-shaped cloud vortex on an IR image.

Here, in the IR range image, a vast cloud vortex in high-altitude stratiform clouds stands out. However, it is completely indistinguishable in visible light. Vortex structures in cloudiness are typically observed in satellite images. Thus, this example illustrates new possibilities for ground-based cloud study using IR cameras.

The image examples presented here do not exhaust the full scope of unusual objects or phenomena that were captured when imaging in the near-IR range. The most interesting cases are those when cloud formations are visible only in IR rays. Moreover, such objects often move very rapidly. Additionally, attention is drawn to the unusual morphology of cloud forms in such images. It is possible that, due to the increased contrast of the images, rather rare cloud forms have been captured on them. These could be, for example, finely dispersed dust clouds, the possible existence of which is pointed out by a number of researchers [30]. In particular, one might note the "ultracirrus" mentioned by Minnaert [6]. In this regard, it is obvious that observations of cloud forms in the near-IR region must be continued.

7. Discussion

Taking into account the fact that in the study of NLC obtaining images in the IR spectral region has not previously been practiced, it is not possible to compare the results of this work with the data of other authors. Moreover, when conducting synoptic observations of NLC, researchers usually limited themselves to the fact of registering such cloudiness, without evaluating the information content (for example, contrast) of the images. And this is quite justified in the case of sufficiently bright cloud fields appearing in the sky. With this approach, the photographic method essentially refines visual observations, imparting to them such crucial qualities as documentation and objectivity.

Although the contrast sensitivity of the human eye is high, there are frequent cases where visual observations do not allow one to confidently judge the presence or absence of NLC in the twilight segment under favorable conditions of its illumination and clear weather. At the same time, discussing the possibility of registering NLC using traditional methods prior to the onset of nautical twilight generally makes no sense.

In this context, the results obtained during the present study provide grounds for an optimistic outlook on the prospects of using near-IR photography to expand capabilities in the study of NLC and other high-altitude cloud formations. This concerns the enhancement of image information content achieved through a significant increase in image contrast.

It should be considered that the potential of the proposed methodology at this stage is far from exhausted. A further increase in the contrast gain for cloud images in the twilight segment is achievable by applying identical ISO values on both the IR and conventional cameras. Naturally, this will require an increase in exposure times when shooting in the IR range, but they will nonetheless remain within acceptable limits. Alongside this, the implementation of cameras featuring sensors with higher sensitivity in the near-IR spectral region becomes a relevant prospect for the future.

8. Conclusion

In order to develop tools and methods for registering NLC during ground-based observations, this work substantiates the possibility of increasing image contrast in the twilight sky segment by transitioning to photographic observations in the near-IR spectral region. In doing so, the discriminability of the structure of low-contrast objects, which is difficult to distinguish when using traditional approaches, is enhanced. The increase in image contrast for diffuse cloud objects is achieved by reducing the background sky brightness.

To implement the new method for registering cloud forms, a Canon 1000D camera was modified by removing the built-in filter in front of the receiver that cuts off IR radiation. Concurrently, filters transmitting only IR radiation of specified wavelengths were mounted on the camera lens [17]. As a result, the sensitivity of the modified camera in the IR spectral region increased by approximately three orders of magnitude [17, 28]. During the summer season of 2025, using the Canon 1000DI camera, systematic observations of the twilight sky segment at wavelengths longer than 850 nm were conducted for the first time. Control images in the visible region were taken simultaneously using a Canon 2000D camera.

Visual matching and comparison of the numerical characteristics of the images in the IR and visible spectral regions revealed interesting results. In particular, in every randomly selected pair of images (IR and visible range), a higher contrast of cloud details was found specifically for the IR images. The relative contrast difference generally amounted to tens, and occasionally more than a hundred percent. Of course, looking ahead, it is interesting to investigate the factors influencing the magnitude of the contrast difference.

It is shown that upon visual comparison of the photographs, the higher image contrast allows for the identification of cloud structures on the IR images that are completely indistinguishable on the images in the visible spectral region [28]. Furthermore, the boundaries of cloud formations on IR images are much sharper, and the structural detailing is much higher than on visible light images. At the same time, the possibility emerges of expanding the temporal range for registering NLC by incorporating a portion of civil twilight into it.

Further refinement of the method for increasing the contrast and quality of cloud images in the twilight sky segment in the IR range is possible by equalizing the sensitivity (ISO) of the main and control cameras. It is possible that some of the cloud formations recorded exclusively in the IR region represent understudied forms of high-altitude clouds. Thus, one can speak of the prospect of applying IR cameras not only for NLC monitoring but also for studying other atmospheric formations whose registration in visible light is problematic [31-34].

Conflicts of interest
The authors declare no conflict of interest.

Author contributions

Conceptualization: A.S.S. and P.I.L.; Methodology: A.S.S., T.B.K. and B.M.U.; Software: T.B.K.; Validation: A.S.S, T.B.K., P.I.L. and B.M.U.; Formal Analysis: A.S.S., T.B.K., P.I.L. and B.M.U.; Investigation: A.S.S. and N.P. S.; Resources: N.P.S..; Data Curation: A.S.S., T.B.K., P.I.L. and B.M.U.; Writing – Original Draft Preparation: A.S.S. and P.I.L.; Writing – Review & Editing: A.S.S.; T.B.K and P.I.L.; Visualization: T.B.K.; Supervision: A.S.S.; Project Administration: B.M.U.; Funding Acquisition: N.P.S.. All authors have read and agreed to the published version of the manuscript.

References

1. M. Gadsden and W. Schröder, Noctilucent Clouds. New York, NY, USA: Springer, 1989.
2. V. A. Bronshten, Noctilucent Clouds and Their Observation: Observation Conditions, Heights and Velocities of Noctilucent Clouds, (in Russian). Moscow, Russia: Redaktsionnaya kollegiya, 1984.
3. P. A. Dalin, V. A. Romeiko, N. N. Pertsev, and V. I. Perminov, “Noctilucent clouds are already 130 years old,” (in Russian), *Priroda*, no. 11(1203), pp. 18-26, 2015, EDN: VHXLIT.
4. S. V. Zvereva, *In a World of Sunshine*, (in Russian). Leningrad, USSR: Gidrometeoizdat, 1988.
5. G. V. Rozenberg, *Twilight*, (in Russian). Moscow, USSR: Fizmatgiz, 1963.
6. M. Minnaert, *Light and Color in the Outdoors*. Springer Science & Business Media, 1995.
7. O. S. Ugolnikov, I. A. Maslov, B. V. Kozelov, and J. M. Dlugach, “Noctilucent cloud polarimetry: Twilight measurements in a wide range of scattering angles,” *Planet. Space Sci.*, vol. 125, pp. 105-113, 2016, https://doi.org/10.1016/j.pss.2016.03.010
8. O. S. Ugolnikov, A. A. Galkin, S. V. Pilgaev, and A. V. Roldugin, “Noctilucent cloud particle size determination based on multi-wavelength all-sky analysis,” Planet. Space Sci., vol. 146, pp. 10-19, 2017. [Online]. Available: http://arxiv.org/abs/1611.00073
9. A. A. Solodovnik, P. I. Leontiev, and P. Dalin, “Studies of the influence of tropospheric factors on the formation of silvery clouds by cartographic method,” *J. Atmos. Sol.-Terr. Phys.*, vol. 200, 2020, Art. no. 105224, https://doi.org/10.1016/j.jastp.2020.105224
10. A. Solodovnik, P. Leontiev, P. Dalin, B. Takenov, and D. Alyoshin, “Seasonal evolution and interseasonal changes in polar mesospheric clouds at high latitudes in the Southern Hemisphere,” *J. Atmos. Sol.-Terr. Phys.*, vol. 226, 2021, Art. no. 105787, https://doi.org/10.1016/j.jastp.2021.105787
11. H. Gao, L. Li, L. Bu, Q. Zhang, Y. Tang, Z. Wang, “Effect of small-scale gravity waves on polar mesospheric clouds observed from CIPS/AIM,” *J. Geophys. Res. Space Phys.,* vol. 123, pp. 4026-4045, 2018, https://doi.org/10.1029/2017JA024855
12. P. Dalin et al., “A case study of long gravity wave crests in noctilucent clouds and their origin in the upper tropospheric jet stream,” *J. Geophys. Res. Atmos.*, vol. 121, no. 23, 2016, https://doi.org/10.1002/2016JD025422
13. N. Shevchuk, N. Pertsev, P. Dalin, V. Perminov, “Wave-induced variations in noctilucent cloud brightness: Model and experimental studies,” *J. Atmos. Sol.-Terr. Phys.*, vol. 203, 2020, Art. no. 105257, https://doi.org/10.1016/j.jastp.2020.105257
14. V. P. Hart et al., “Investigating gravity waves in polar mesospheric clouds using tomographic reconstructions of AIM satellite imagery,” *J. Geophys. Res. Space Phys.*, vol. 123, pp. 955-973, 2018, https://doi.org/10.1002/2017JA024481
15. A. Solodovnik, A. Baibusinova, D. Kudabaeva, “Dynamics of the development of the field of noctilucent clouds in the northern Hemisphere in the period 2013-2020,” *Bull. KazNTU*, no. 4(140), pp. 138-144, 2020.
16. P. Dalin et al., “Ground-based observations of noctilucent clouds with a Northern Hemisphere network of automatic digital cameras,” *J. Atmos. Sol.-Terr. Phys.*, vol. 70, pp. 1460-1472, 2008. https://doi.org/10.1016/j.jastp.2008.04.018
17. A. Solodovnik, R. Zyryanov, P. Leontyev, B. Useinov, E. Gololobova, and P. Zhuravlev, “Experience of noctilucent clouds registering in the near infrared spectrum region,” *Phys. Sci. Technol.*, vol. 11, no. 1-2, 2024. https://doi.org/10.26577/phst2024v11i1a10
18. A. A. Solodovnik, P. I. Leontyev, B. M. Useinov, A. D. Kadyrmin, and R. O. Zyryanov, “Application of electronic receivers for recording infrared images of celestial phenomena at the CAR of the NKU,” *Phys. Sci. Technol.*, vol. 10, no. 1-2, 2023. https://doi.org/10.26577/phst.2023.v10.i1.07
19. A. Sheverdin, “Technological innovations of OmniVision CMOS cameras: An optimal choice for high-volume applications,” (in Russian), *Komponenty i Tekhnologii*, no. 1, 2008.
20. Canon Inc., *Canon EOS 2000D User Manual*, (in Russian). Tokyo, Japan: Canon Inc., 2017.
21. S. Qiu et al., “Solar-induced 27-day modulation on polar mesospheric cloud (PMC), based on combined observations from SOFIE and MLS,” *Front. Astron. Space Sci.*, vol. 10, 2023, Art. no. 1168841, https://doi.org/10.3389/fspas.2023.1168841
22. V. I. Perminov et al., “Response of the mesopause region airglow to short-period changes in solar activity,” (in Russian), *Geomagn. Aeron.,* vol. 63, no. 1, pp. 63-72, 2023.
23. A. Sarsembayeva, L. Ryssaliyeva, F. Belissarova, and A. Sarsembay, “Solar magnetic activity and its terrestrial impact through correlations with drought indices,” *Phys. Sci. Technol*., vol. 12, no. 1-2, pp. 38-44, 2025. https://doi.org/10.26577/phst20251214
24. Yu. I. Golub and F. V. Starovoitov, “Study of local contrast estimates of digital images in the absence of a reference,” (in Russian), *Syst. Anal. Appl. Inform.*, no. 2, pp. 4-11, 2019, https://doi.org/10.21122/2309-4923-2019-2-4-11
25. S. A. Kadnichanskiy, “Contrast estimation of digital aerial photographs and satellite images,” (in Russian), *Geod. Cartogr.,* no. 3, pp. 46-51, 2018, https://doi.org/10.22389/0016-7126-2018-933-3-46-51
26. “Numerical characteristics of the image. The tonal range,” MyPresentation.ru. Accessed: Mar. 4, 2023. [Online]. Available: https://mypresentation.ru/presentation/chislovye-xarakteristiki-izobrazhenij

27. "Processing of images and video files. How to read, understand and recognize the histogram of an image," Rugraphics.ru. Accessed: Mar. 4, 2023. [Online]. Available: https://rugraphics.ru/photoshop/kak-chitat-ponimat-raspoznavat-gistogrammu

28. T. B. Kasenov, "Evaluation of image contrast when working with an infrared camera EOS Canon-1000D," (in Russian), in Proc. Int. Sci.-Pract. Conf. Youth and Science-2025: Modern Challenges and Scientific Approaches to Solving Them, Dedicated to the 100th Anniversary of Evnei Arstanovich Buketov, Petropavlovsk, Kazakhstan, Apr. 9, 2025, pp. 391–396, EDN: AIQXRA.

29. T. Ferreira and W. S. Rasband, "ImageJ User Guide—IJ 1.46," ImageJ.net, 2010-2012. [Online]. Available: https://imagej.net/ij/docs/guide/

30. A. V. Kislov and G. V. Surkova, *Climatology: Textbook.* Moscow, Russia: INFRA-M, 2022.

31. A. A. Solodovnik, R. A. Kleksin, P. I. Leontyev, B. M. Useinov, A. G. Markova, and S. A. Kassimova, "Revealing the noctilucent cloud fields structure by software processing of satellite images," *Phys. Sci. Technol.*, vol. 12, no. 1-2, pp. 4-13, 2025. https://doi.org/10.26577/phst20251211

32. A. A. Solodovnik, B. M. Useinov, T. B. Kassenov, P. L. Zhuravlev, and E. A. Solodovnik, "Experience of using an infrared camera in the study of astronomical objects," *Recent Contrib. Phys.*, no. 1(96), pp. 14-22, 2026.

33. A. A. Solodovnik, P. I. Leontyev, S. A. Sartin, B. M. Useinov, D. V. Alyoshin, and P. Dalin, "Physical bases of meteor registration methods and the instrument complex of the NKU Observatory," *Int. J. Math. Phys.,* vol. 13, no. 2, 2022. https://doi.org/10.26577/ijmph.2022.v13.i2.04A

34. P. Razzhivalov, N. Korobova, and S. Shatalova, "Earth sensing capabilities yesterday and today," *Phys. Sci. Technol.,* vol. 8, no. 1-2, pp. 26-34, 2021. https://doi.org/10.26577/phst.2021.v8.i1.03

Information about the authors:

Andrey Solodovnik – Candidate of Physico-Mathematical Sciences, Professor at the M. Kozybayev North Kazakhstan University (Petropavlovsk, Kazakhstan, e-mail: asolodovnik@ku.edu.kz).

Timur Kassenov – Master's student at the M. Kozybayev North Kazakhstan University (Petropavlovsk, Kazakhstan, e-mail: timur.kasenov.2002@mail.ru).

Pavel Leontyev – Candidate of Physico-Mathematical Sciences, Associate professor at the M. Kozybayev North Kazakhstan University (Petropavlovsk, Kazakhstan, e-mail: pleontyev@mail.ru, pleontiev@ku.edu.kz).

Beibut Useinov (corresponding author) – Candidate of Physico-Mathematical Sciences, Professor at the M. Kozybayev North Kazakhstan University (Petropavlovsk, Kazakhstan, e-mail: buseinov@gmail.com).

Nadezhda Solodovnik – research associate at the M. Kozybayev North Kazakhstan University (Petropavlovsk, Kazakhstan, e-mail: npsolodovnik@mail.ru).